

Cite this: DOI:00.0000/xxxxxxxxxx

## Supporting Material: Self-assembly of active bifunctional Brownian particles

Caterina Landi <sup>a</sup>, John Russo <sup>b</sup>, Francesco Sciortino <sup>b</sup>, Chantal Valeriani <sup>a</sup>

Received Date

Accepted Date

DOI:00.0000/xxxxxxxxxx

### 1 State diagrams at different temperatures

We have also studied the system at two intermediate temperatures:  $T = 0.08$  and  $T = 0.09$ . Hereby, Fig. 1 reports the corresponding  $\rho$  versus  $Pe$  state diagrams.

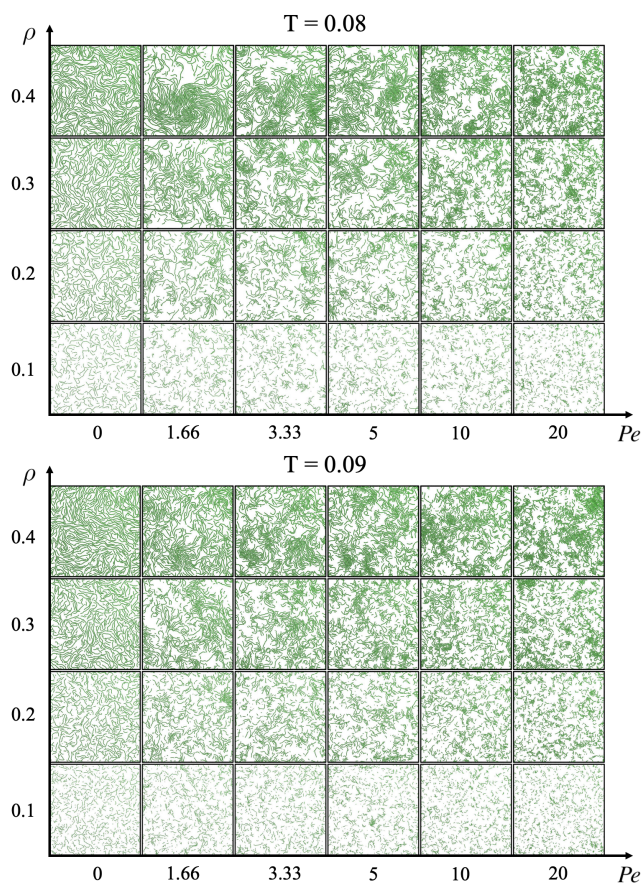


Fig. 1 Steady state configurations, as a function of activity and density, at temperature  $T = 0.08$  (top panel) and  $T = 0.09$  (bottom panel). Activity increases horizontally (from left to right) and density increases vertically (from bottom to top).

### 2 Definition of the system's steady state

We have defined the steady state as the state where the total potential energy (or the total number of bonds) is stationary as a function of time. We cannot exclude that at longer time intervals a phase separation could occur, but our evidence suggests that the system enters a stationary state where all static quantities (such as the chain length distribution, cluster size distribution or the structure factor) do not change over time.

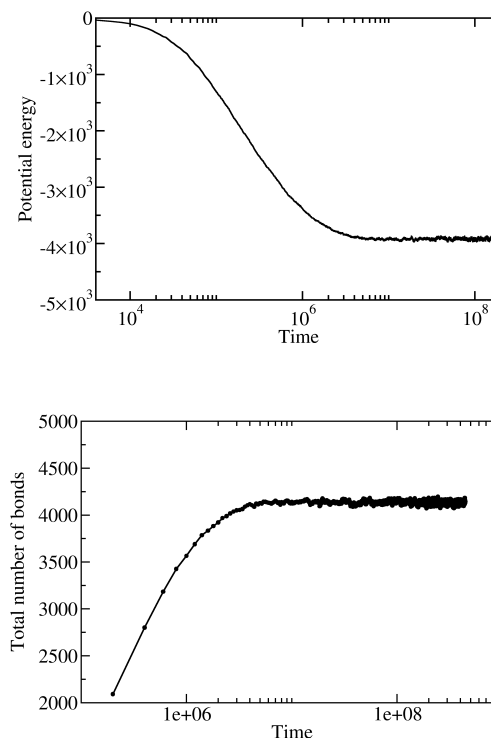


Fig. 2 Top) Total potential energy as a function of time. Bottom) Total number of bonds as a function of time. Both panels represent the system at temperature  $T = 0.09$ , density  $\rho = 0.4$  and Péclet number  $Pe = 20$ .

Fig. 2 shows the total potential energy (top panel) and the total number of bonds (bottom panel) as a function of time for the system at temperature  $T = 0.09$ , density  $\rho = 0.4$  and Péclet number  $Pe = 20$ .

In this example, the system reaches a steady state for times longer than  $5 \times 10^6$  steps. The analysis of the manuscript will be conducted averaging over steady state configurations after  $10^8$  steps.

### 3 Chain length and cluster size distributions at different densities and temperatures

To provide additional insight, we have also studied the chain length and cluster size distributions at two densities lower than the ones presented in the main text,  $\rho = 0.2$  and  $\rho = 0.1$ . Figure 3 shows the chain length distributions and cluster size distributions at  $\rho = 0.2$  and  $\rho = 0.1$  at  $T=0.1$  and for different Peclet values.

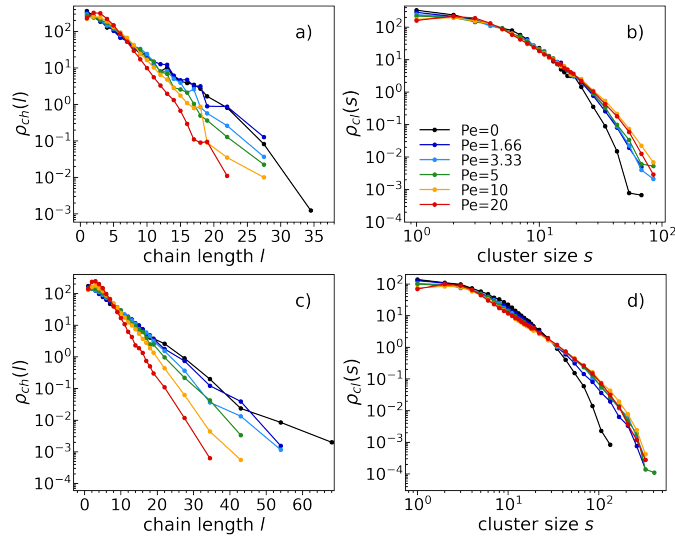


Fig. 3 Chain length distributions (left panels) and cluster size distributions (right panels) for the system at temperature  $T = 0.1$ , density  $\rho = 0.1$  (top) and  $\rho = 0.2$  (bottom), and all studied Péclet numbers (see legend).

At these densities, the chain length distributions (Fig. 3 a, c) does not show a significantly different behavior as compared to those reported in the main text. This is confirmed by the results for the cluster size distributions (Fig. 3 b, d). As suggested in the main text, the system does not percolate at low density: in this case, clusters coincide with chains and the cluster size distributions decay exponentially.

For the sake of completeness, we also studied the chain length and cluster size distributions at three lower temperatures:  $T = 0.9$  (Fig. 4),  $T = 0.8$  (Fig. 5), and  $T = 0.7$  (Fig. 6).

For both the chain length distributions and the cluster size distributions, we observed the behavior described in the main text. However, as the temperature decreases, results become noisier because more time is required to reach a steady state, and fewer configurations are available for averaging.

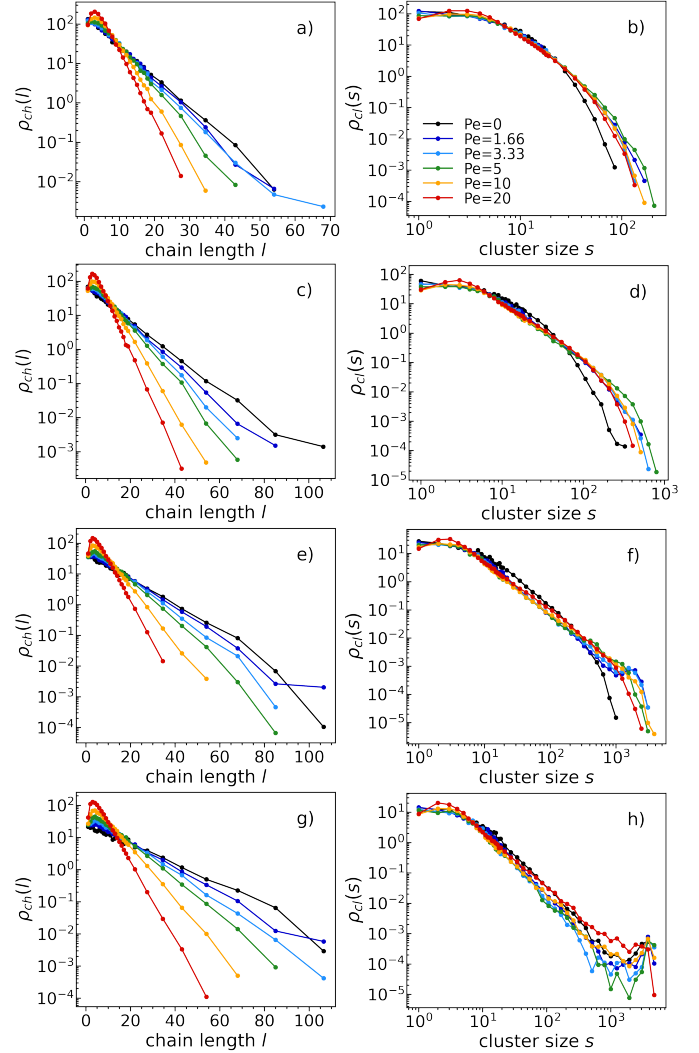


Fig. 4 Chain length distributions (left panels) and cluster size distributions (right panels) at temperature  $T = 0.09$ . Density increases from top to bottom:  $\rho = 0.1$  a) and b),  $\rho = 0.2$  c) and d),  $\rho = 0.3$  e) and f), and  $\rho = 0.4$  g) and h). See legend for the studied Péclet numbers.

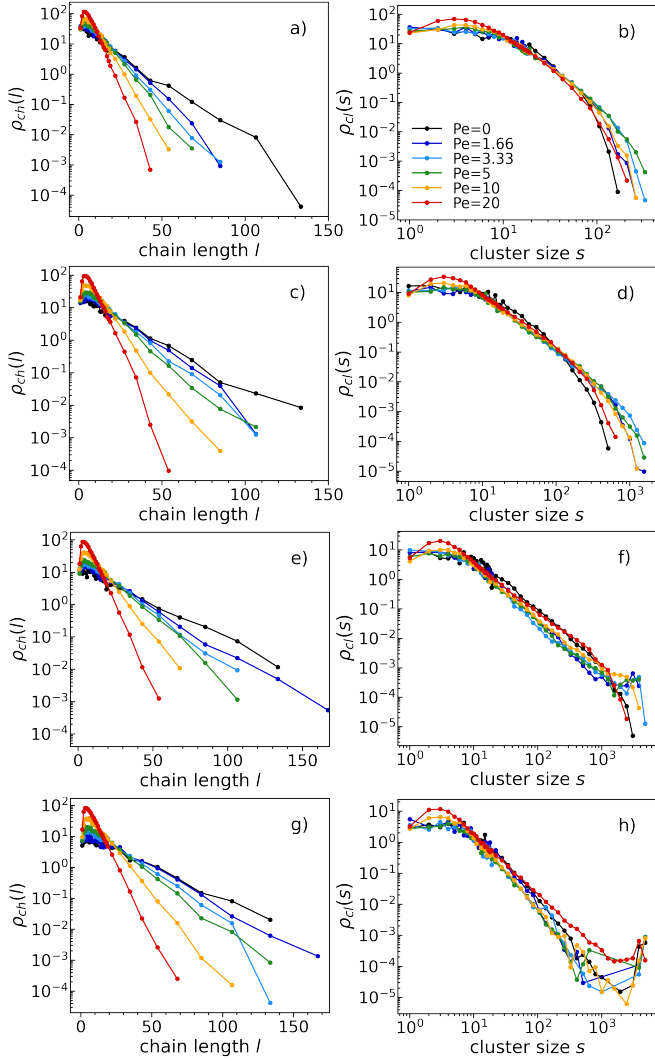


Fig. 5 Chain length distributions (left panels) and cluster size distributions (right panels) at temperature  $T = 0.08$ . Density increases from top to bottom:  $\rho = 0.1$  a) and b),  $\rho = 0.2$  c) and d),  $\rho = 0.3$  e) and f), and  $\rho = 0.4$  g) and h). See legend for the studied Péclet numbers.

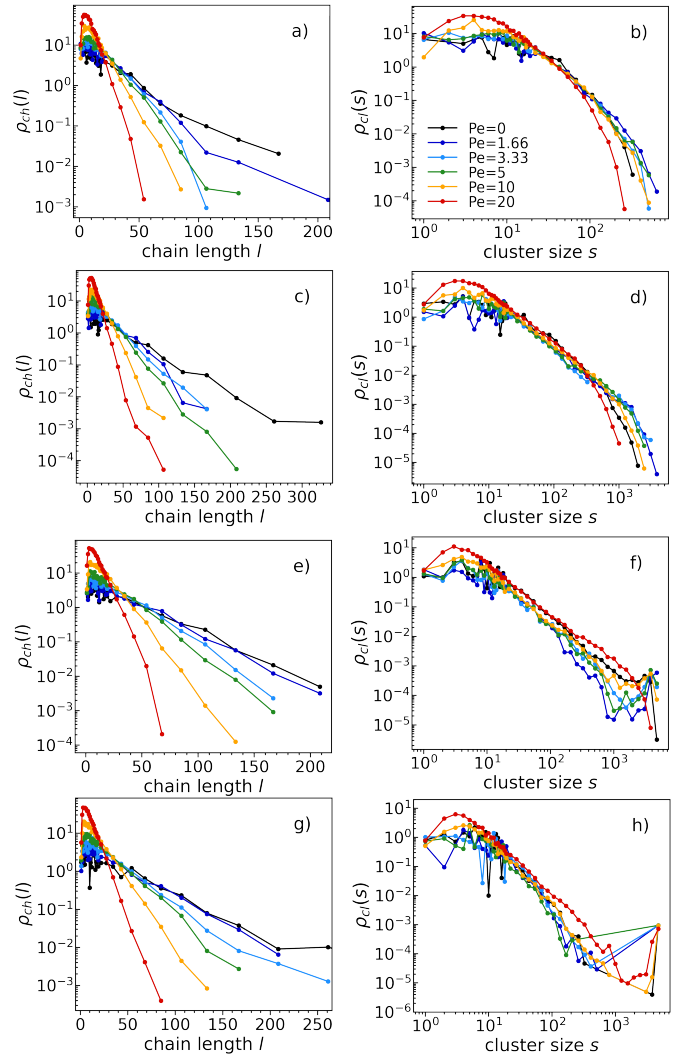


Fig. 6 Chain length distributions (left panels) and cluster size distributions (right panels) at temperature  $T = 0.07$ . Density increases from top to bottom:  $\rho = 0.1$  a) and b),  $\rho = 0.2$  c) and d),  $\rho = 0.3$  e) and f), and  $\rho = 0.4$  g) and h). See legend for the studied Péclet numbers.

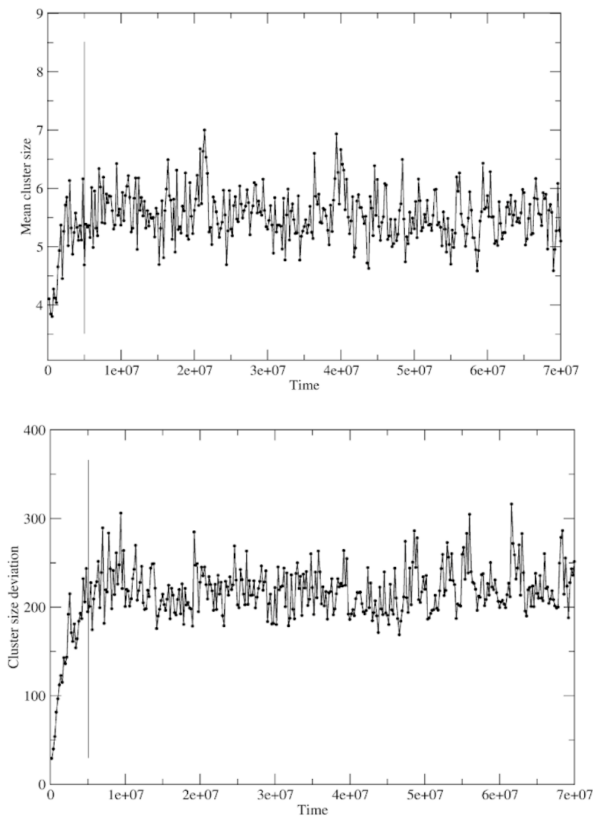


Fig. 7 Mean cluster size and its deviation at temperature  $T=0.09$ , density  $\rho = 0.4$  and Péclet number  $Pe = 20$ . The vertical black lines at  $5 \times 10^6$  are included as a visual guide.

We have also computed the mean cluster size and its deviation, which are now shown as functions of time in Fig. 7 for the system at temperature  $T=0.09$ , density  $\rho = 0.4$  and Péclet number  $Pe = 20$ . According to these two plots, the system reaches a stationary state on a timescale consistent with the one indicated by the plots of the total potential energy and the total number of bonds.

## 4 Spiral state

For the sake of completeness, we more thoroughly analyze the spiral state.

### 4.1 Computing the distribution of the average turning number

We have computed the probability distribution of the average turning number  $\chi$  for the system at temperature  $T = 0.07$  and Péclet number  $Pe = 1.66$ , reported in Fig. 8.

As shown in the figure, the main peak is close to  $\chi = 0$ , which corresponds to the elongated state. Increasing the density, we observe the rise of a small peak towards  $\chi = 1$ , indicating a weakly wound-up spirals regime.

### 4.2 Computing the spiral number

We underline that the definition of the turning number given in <sup>1</sup> is equivalent to the definition of the spiral number given in <sup>2</sup>,

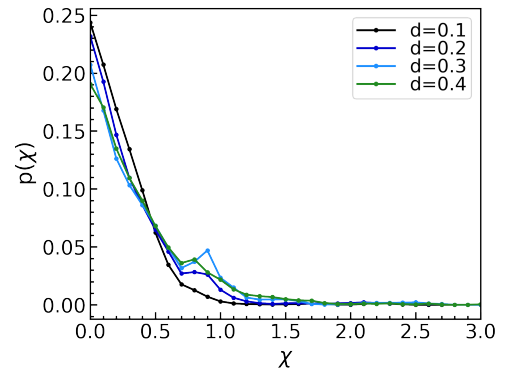


Fig. 8 Probability distribution of the average turning number  $\chi$  at temperature  $T = 0.07$  and Péclet number  $Pe = 1.66$ .

which corresponds to:

$$s_i = \frac{\alpha_i - \alpha_0}{2\pi} \quad (1)$$

where  $\alpha_i$  is the bond orientation of the last monomer and  $\alpha_0$  of the first one. As for the turning number (see main text), we are interested in the absolute value, and have averaged over all chains of the system and some steady state configurations  $s = \langle \sum_{i=1}^{\bar{N}} |s_i| / \bar{N} \rangle$ .

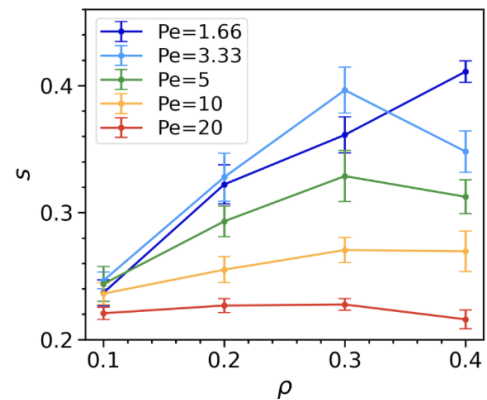


Fig. 9 Average spiral number  $s$  as a function of density  $\rho$  at temperature  $T = 0.07$  and all Péclet numbers different from zero which are studied at this temperature (see legend).

As shown in the figure 9, the values obtained for the spiral number coincide with those obtained for the turning number and reported in the main text.

### 4.3 Structure factor

To compare with the results presented in the main text, we studied the structure factor of the system at temperature  $T = 0.07$  and density  $\rho = 0.4$ , where the system is in a spiral state.

Fig. 10 shows the structure factor of the system at the temperature and density just mentioned and for all Péclet numbers. Interestingly, do not observe any relevant signals of the spirals from the calculation of the structure factor.

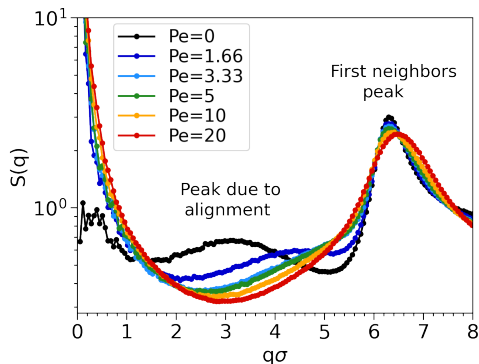


Fig. 10 Structure factors at temperature  $T = 0.07$ , density  $\rho = 0.4$ , and all studied Péclet numbers (see legend).

## 5 Crystal state

To provide a more comprehensive overview of the crystalline clustering process, which is a two-step self-assembly process (first particles self-assemble into chains, then chains self-assemble into a cluster), we present the local density distribution computed for the centers of mass of the chains in the crystalline configurations (Fig. 11 a), together with a typical snapshot showing their locations in the crystalline cluster (Fig. 11 b).

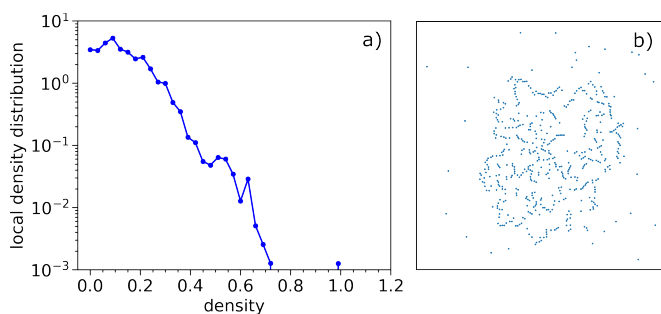


Fig. 11 a) Local density distribution computed for the centers of mass of the chains in the crystalline configuration. b) Positions of the centers of mass of the chains in the crystalline configuration.

Both panels support the fact that chains are in an aggregated state. The local density distribution presents non-zero values for mid-range densities, other than just small densities (Fig. 11 a). Moreover, the centers of mass are not uniformly distributed in space (Fig. 11 b). However, chains cannot aggregate more due to excluded volumes.

### 5.1 Zooming in the state diagram: the crystal phase region

To qualitatively sketch the boundaries of the crystalline region in the  $\rho$ - $Pe$  plane, we have performed a series of simulations around the crystal phase. The results are presented in the  $\rho$ - $Pe$  state diagram of Figure 12.

Fig. 12 shows the boundaries of the crystal phase (indicated with a red line) for higher values of activity.

## Notes and references

- 1 G. Janzen and D. A. Matoz-Fernandez, *Soft Matter*, 2024, **20**, 6618–6626.

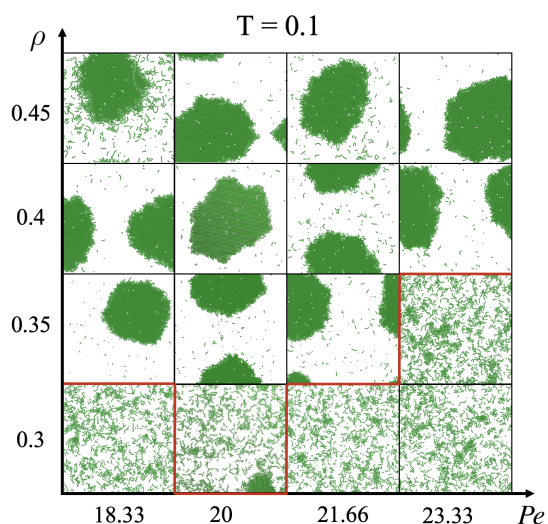


Fig. 12 Steady state configurations as a function of activity and density, at temperature  $T = 0.1$ . Activity increases horizontally (from left to right) and density increases vertically (from bottom to top). The red line indicates a qualitative estimate of the phase boundaries.

- 2 R. E. Isele-Holder, J. Elgeti and G. Gompper, *Soft Matter*, 2015, **11**, 7181–7190.